Journal of Alloys and Compounds, 207/208 (1994) 340–348
JALCOM 3075

Light-metal base amorphous alloys containing lanthanide metal

Akihisa Inoue and Tsuyoshi Masumoto
Institute for Materials Research, Tohoku University, Sendai 980 (Japan)

Abstract

Light-metal base amorphous alloys with high specific strength and good corrosion resistance were produced in Al- and Mg-based systems containing lanthanide (Ln) as an essential solute element for glass formation. The amorphous alloy systems were composed of Al–Ln, Al–Ln–TM, Mg–Ln, Mg–Ca–Ln and Mg–Ln–TM (TM = transition metal). The addition of TM was very effective for the extension of their glass formation ranges. The highest tensile strength (σ_f) reaches 1250 MPa for the Al-based alloys and 830 MPa for the Mg-based alloys. The Mg-based alloys have a large glass-forming capacity which enables the production of an amorphous phase by a metallic mold casting method. The extrusion of the Al-based amorphous powders at temperatures above crystallization temperature caused the formation of high strength materials with finely mixed structure consisting of dispersed intermetallic compounds in an Al matrix. The highest values of σ_f and the fatigue limit are as high as 940 and 330 MPa, respectively, at room temperature and 520 and 165 MPa at 473 K. The extruded Al–Ni–Mm alloys have been used as machine parts and subsequent further development as practical materials is expected.

1. History of the development of amorphous alloys in Al–Ln and Mg–Ln (Ln=lanthanide metal) systems

By utilizing the increase in strength and ductility resulting from the formation of an amorphous phase for metallic materials, the development of high strength materials combined with ductility has very actively been carried out for the last two decades. Particularly, great effort has been devoted to the production of Al-based amorphous alloys, with the aim of utilizing a high strength material with light weight [1,2]. However, there have been no successful data on the production of Al-based amorphous alloys with high tensile strength and good bending ductility, although the formation of an amorphous single phase in Al-based alloys containing more than 50 at.% Al has been reported in A–Ln–M–B (M = Fe, Co or Ni) systems [3]. The first evidence of an Al-based amorphous alloy with high strength and good bending ductility was obtained in an Al-Ni-Si system in 1987 [4]. Subsequently, Al-based amorphous alloys with high strength and good bending ductility have been reported to be obtained in Al–ETM–LTM alloy systems [5]. In the investigation on the effect of these solute elements on the glass-formation tendency, mechanical strength and thermal stability of Al-based amorphous alloys in Al–TM–Si [6], Al–TM–Ge [6] and Al–ETM–LTM [5] systems, we have derived an empirical rule in which the Al-based amorphous phase is formed in the system with strong attractive bonding nature between Al and solute elements.

Based on this empirical rule, we have investigated the Al–Ln system because the attractive bonding nature was thought to be the largest for Al–Ln pairs. As a result, we have succeeded for the first time in producing an amorphous alloy with high tensile strength in Al–Ln [7–9] and Al–Ln–TM [10,11] systems. Subsequently, by taking the similarity of the bonding nature between Al–Ln and Mg–Ln atomic pairs into consideration, we also succeeded in producing Mg-based amorphous alloys in Mg–Ln–TM [12,13] and Mg–Ln [14] systems by melt spinning. This paper aims to review very briefly our recent results on the formation and fundamental properties of the Al- and Mg-based amorphous alloys containing Ln elements as an essential solute element for glass formation, along with the data on Al- and Mg-based amorphous alloys without Ln elements.

2. Al- and Mg-based amorphous systems

When the melt-spun ribbon with a thickness of about 20 μm in Al- and Mg-based alloys is produced by a single roller melt spinning technique, the alloy compositions at which an amorphous single phase is formed can be divided into two categories of metal–metal and metal–metalloid [15], as summarized in Table 1. In these alloy systems, the important alloys exhibiting high

SSDI 0925-8388(93)03075-T

TABLE 1. Al- and Mg-based amorphous alloys produced by single roller melt spinning

Alloy	Metal–metal system	Metal–metalloid system
Al base	Al–Ln Al–Ln–TM, Al–ETM–LTM, Al–LTM–LTM	Al–B–TM, Al–Si–TM, Al–Ge–TM
Mg base	Mg–Ca, Mg–Ni, Mg–Cu, Mg–Zn, Mg–Y Mg–Ca–M, Mg–Sr–M, Mg–Ca–Ln, Mg–Ni–Ln, Mg–Cu–Ln, Mg–Zn–Ln, Mg–Ln–Ln	Mg–Ca–Si, Mg–Ca–Ge, Mg–Ni–Si, Mg–Ni–Ge, Mg–Cu–Si, Mg–Cu–Ge, Mg–Zn–Si, Mg–Zn–Ge

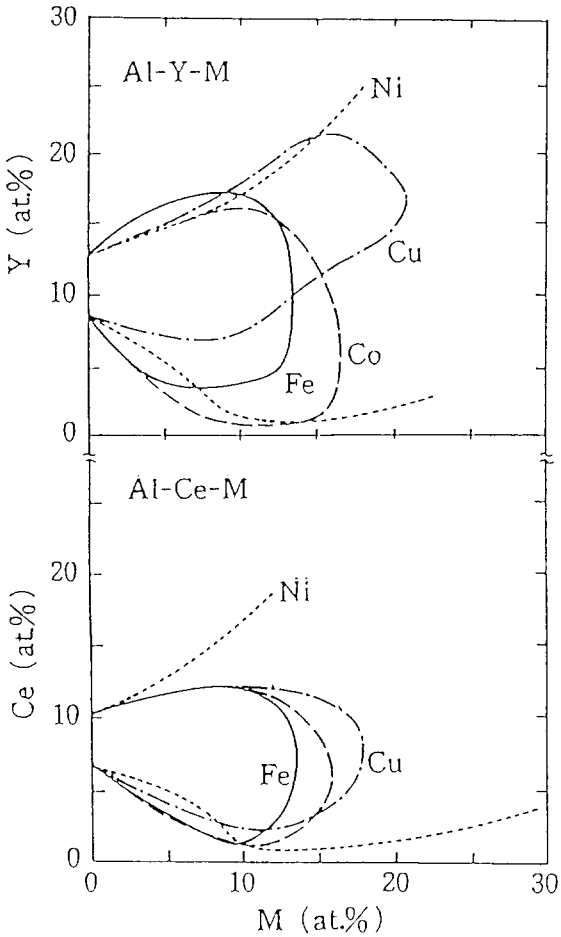

Fig. 1. Composition range for formation of the amorphous phase in Al–Y–M and Al–Ce–M (M = Fe, Co, Ni or Cu) systems by melt spinning.

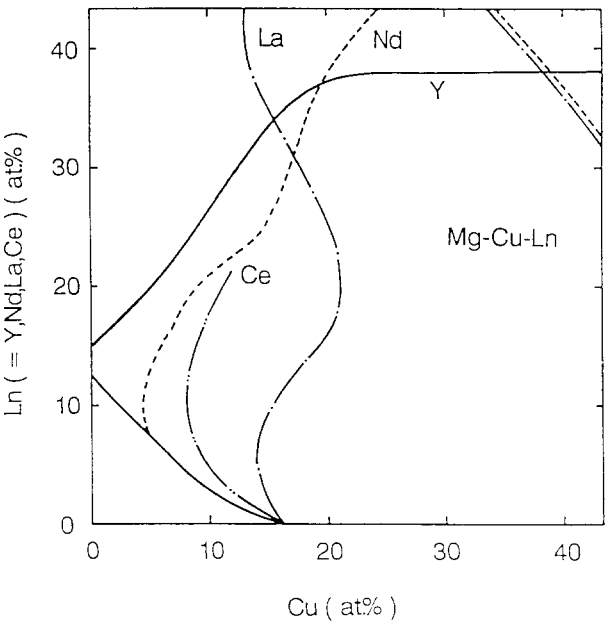

Fig. 2. Composition range for formation of the amorphous phase in Mg–Cu–Ln (Ln = Y, La, Ce or Nd) systems by melt spinning.

strength are Al–Ln–TM (Ln = lanthanide metal, TM = transiton metal) [10,11,15–17], Mg–M–Ln (M = Ni, Cu, Zn) [12,13] and Mg–Ln–Ln [18] containing Ln elements as a solute element.

As examples, Figs. 1 and 2 show the composition range in which an amorphous single phase is formed in Ln-containing Al–Ln–TM (Ln = Y, Ce, TM = Fe, Co, Ni, Cu) and Mg–Cu–Ln (Ln = Y, La, Ce, Nd) systems, respectively. Both the alloy systems have very wide glass-formation ranges. In addition, metastable supersaturated fcc-Al or hcp-Mg solution is formed at the lower solute concentration side compared to that of the glass-formation range [19].

The feature of these amorphous alloys is due to the existence of Ln elements. The following points can be described as the effect of Ln elements. The atomic pairs of Al–Ln and Mg–Ln have large atomic size ratios and large negative heats of mixing. It is therefore presumed that the atomic diffusivity in the liquid supercooled below the melting temperature is low enough to suppress the nucleation and growth reaction of a crystalline phase, leading to a large glass-forming ability in the Al- and Mg-based alloys containing Ln elements. Based on this information, we can derive the concept that the finding of an alloy with a larger glass-forming ability seems to be possible by combining Al or Mg with an element having an atomic size ratio above 10% and a large negative heat of mixing against Al or Mg.

3. Mechanical properties

Table 2 summarizes the tensile fracture strength (σ_f), Young's modulus (E) and Vickers hardness (H_v) for Al- and Mg-based amorphous alloys containing Ln elements [10,12,14,20], along with tensile elongation ($\epsilon_{t,f} = \sigma_f/E$) and compressive yield strain ($\epsilon_{c,y} \approx 9.8H_v/3E$). As seen in the table, the highest σ_f value is 1250 MPa for $Al_{85}Y_8Ni_5Co_2$ and 830 MPa for $Mg_{80}Y_5Ni_{15}$. These values are about two to three times

TABLE 2. Mechanical properties of Al- and Mg-based amorphous alloys

Alloy (at.%)	σ_f (MPa)	E (GPa)	H_v	$\epsilon_{t,f}=\sigma_f/E$	$\epsilon_{c,y}\equiv 9.8H_v/3E$
$Al_{87}Y_8Ni_5$	1140	71.2	300	0.016	0.014
$Al_{87}La_8Ni_5$	1080	88.9	260	0.012	0.010
$Al_{84}La_6Ni_{10}$	1010	83.6	280	0.012	0.011
$Al_{85}Ce_5Ni_{10}$	935	59.4	320	0.016	0.018
$Al_{85}Ni_5Y_8Co_2$	1250	74.0	350	0.017	0.015
$Al_{85}Ni_5Y_7Co_3$	1140	71.2	340	0.016	0.016
$Mg_{80}Y_5Ni_{15}$	830	46.1	224	0.018	0.016
$Mg_{85}Y_{10}Cu_5$	800	44.3	205	0.018	0.015

higher than the highest values [21] of commercial Al- and Mg-based crystalline alloys. The tensile fracture of these amorphous alloys in a ribbon form occurs along the maximum shear plane which is declined by 45-55° to the tensile axis. The fracture surface consists of a smooth region caused by the shear sliding and a vein region caused by catastrophic tensile fracture after the shear sliding. Furthermore, the amorphous ribbon can be bent through 180° and cold-rolled up to a reduction in area above 50% without fracture. Such deformation and fracture behaviors are just the same as those for other transition-metal based amorphous alloys, being independent of the existence of the Ln elements.

Since the amorphous structure is in a thermodynamically metastable state, the subsequent heating causes crystallization, leading to the loss of characteristics typical for an amorphous alloy. Consequently, it is necessary to look for an amorphous alloy exhibiting a high crystallization temperature (T_x). Similar to σ_f, E and H_v, T_x increases with increasing solute content from 500 to 720 K for the Al–Ln–TM system and from 420 to 600 K for the Mg–M–Ln system. The ratio of these highest T_x values to the melting temperature of Al or Mg is 0.77 for the Al base and 0.64 for the Mg base, indicating that these amorphous alloys have rather high thermal stability. The high stability is due to the formation of the amorphous structure with highly attractive bonding nature and large atomic size ratios among Ln, TM and Al or Mg atoms.

4. Appearance of supercooled liquid before crystallization and its thermal stability

The stability against crystallization for the Al- and Mg-based amorphous alloys subjected to continuous heating is described in Section 3. Here, it is important to introduce the fact that the Al- and Mg-based amorphous alloys have a feature in which the amorphous solid changes to a supercooled liquid at temperatures below T_x. The temperature at which the transition occurs is called the glass transition temperature (T_g) and the viscosity at T_g is of the order 10^{12} Pa s. The temperature interval between T_g and T_x, ΔT_x ($=T_x-T_g$) corresponds to the supercooled liquid region and the viscosity in the region is well below 10^{12} Pa s. That is, the atomic diffusivity in this temperature region is extremely large and an internal equilibrium state is achieved because of very short relaxation times.

ΔT_x of the Al–Ln–TM amorphous alloys is larger than 20 K in the composition ranges of 5–10% Ln and 3–12% Ni or Co and the largest value is 38 K for $Al_{85}Y_8Ni_5Co_2$ [19,22]. On the other hand, as shown in Fig. 3, the ΔT_x value of Mg–Cu–Y amorphous alloys is above 40 K in a wide composition range of 15–40% Cu and 7–23% Y and the largest value reaches 69 K for $Mg_{65}Cu_{25}Y_{10}$. Similar large ΔT_x values above 40 K have also been observed [23] in other Mg–M–Ln amorphous alloys such as Mg–Cu–Ln and Mg–Ni–Ln, etc. It is very interesting that the Mg-based amorphous alloys have a large ΔT_x, above 40 K, in wide composition ranges. This result suggests that the Mg-based alloys have a unique disordered structure in order to suppress the nucleation and growth of a crystalline phase even in the supercooled liquid with easy diffusivity of atoms. The constituent elements in these alloys have large negative heats of mixing and atomic size ratios above 10%. It is therefore presumed that these amorphous alloys have a strong bonding nature among the constituent elements as well as a high degree of dense random packed state. As a result, the long-range diffusivity in the amorphous phase decreases and the phase transition to a crystalline state is suppressed because of the necessity for redistribution of the constituent elements for nucleation and growth reactions of crystallization. The presumption that the amorphous structure in the Mg–M–Ln system has a highly dense random packed state has been confirmed [24,25] by the anomalous X-ray diffractometry analysis.

As described above, the finding that a wide supercooled liquid region exists in Al- and Mg-based alloys has an extremely important significance. That is, the supercooled liquid in the ΔT_x region has a large flowability (low viscosity). This feature implies that amorphous bulk can be produced either by warm consolidation or pressing of amorphous powders.

5. Production of high strength amorphous bulk in Mg-based systems by a metallic mold casting method

As described in Section 4, the amorphous alloys in the Mg–M–Ln system have a large ΔT_x value reaching 70 K. The large ΔT_x value indicates that the supercooled

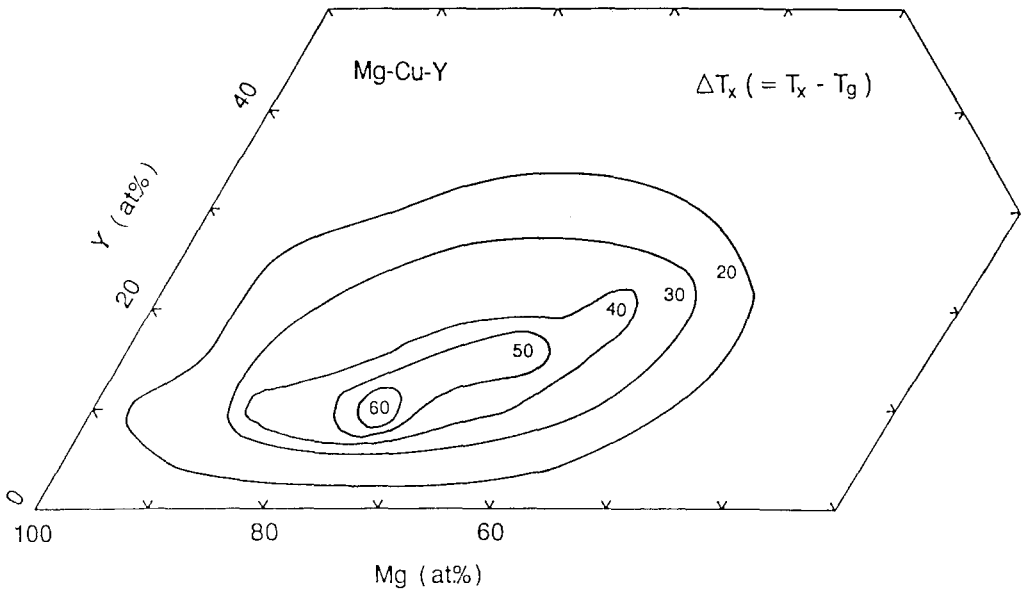

Fig. 3. Compositional dependence of ΔT_x ($=T_x-T_g$) for amorphous Mg–Cu–Y alloys.

liquid has a high thermal stability against crystallization. This also implies that the liquid supercooled at temperatures below the melting temperature has a large resistance against the transformation to a crystalline phase. It is therefore expected that the alloys with a large ΔT_x value have a large glass-forming ability.

Based on this expectation, the production of Mg-based amorphous alloys was tried by the high pressure die casting method in which a molten alloy is cast into a copper mold with a high applied pressure of 63 MPa. As a result, bulky amorphous Mg base alloys in cylindrical and sheet form can be produced and the surface morphology of the cast Mg-based amorphous alloys is shown in Fig. 4. The maximum diameter (D_c) of the amorphous cylinder is closely related to the ΔT_x value. For instance, the D_c value is 3.0 mm for $Mg_{80}Y_{10}Cu_{10}$ with $\Delta T_x=21$ K and above 9.0 mm for $Mg_{65}Y_{10}Cu_{25}$ with $\Delta T_x=69$ K. There is a clear tendency for the D_c value to increase with increasing ΔT_x.

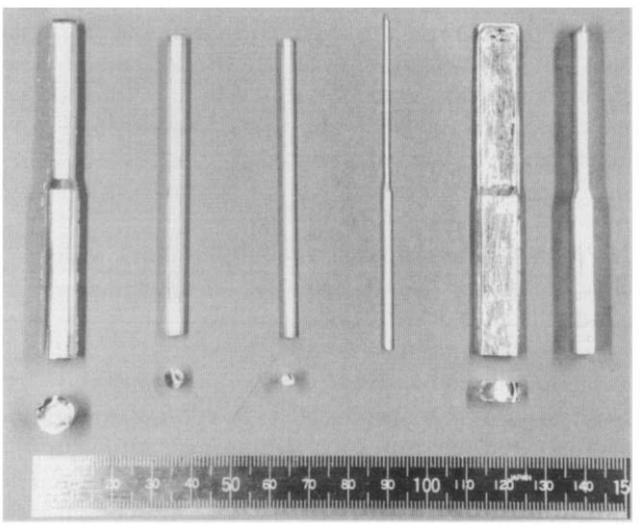

Fig. 4. Surface appearance of $Mg_{65}Y_{10}Cu_{25}$ samples in cylindrical and sheet forms produced by high pressure die casting.

According to the experiments [26] on σ_f of the cylindrical $Mg_{80}Y_{10}Cu_{10}$ amorphous alloy with a diameter of 1.5 mm, σ_f is 790 MPa at room temperature and remains almost unchanged at temperatures below 373 K. With further increasing temperature, the σ_f decreases significantly and is as low as about 20 MPa near T_g. Although the tensile elongation is 0.2% at room temperature, it increases to 10% at 383 K and rapidly above 100% at 453 K near T_g. Thus, the Mg-based amorphous bulk has high strength and good ductility at temperatures below 373 K. It has further been confirmed that the tensile fracture behavior and the fracture surface appearance of the amorphous bulk are nearly the same as those for the amorphous ribbon produced by the single roller melt spinning method.

6. Remarkable increase in tensile strength of Al-based amorphous alloys by dispersion of nanoscale fcc-Al particles

It is generally known [27] that an amorphous alloy becomes remarkably brittle by the precipitation of a crystalline phase. Recently, we have found [28–31] a novel phenomenon that Al–Y–Ni and Al–Ce–Ni amorphous alloys containing homogeneously dispersed Al particles with ultrafine sizes of 3–10 nm exhibit tensile strengths which are about 1.5 times as high as those for the amorphous single phase alloys with the same alloy composition.

As an example, Fig. 5 shows the bright-field electron micrographs and selected-area diffraction patterns of an $Al_{88}Y_2Ni_9Fe_1$ ribbon produced at rotation speeds of 5000 rpm (83 s^{-1}) and 2000 rpm (33 s^{-1}) by the single roller melt spinning technique with a copper wheel of 20 cm in diameter. The as-quenched structure consists of an amorphous single phase at 5000 rpm and an amorphous phase containing homogeneously dispersed Al particles with a size of about 5 nm at 2000 rpm. The volume fraction of the Al phase (V_f) was evaluated to be about 19% from the change in the heat of exothermic reaction due to the precipitation of the Al phase on the DSC curve. Figure 6 shows the change in the mechanical properties as a function of V_f for the melt-spun $Al_{88}Y_2Ni_9M_1$ (M = Mn, Fe or Co) alloys. Both σ_f and ϵ_f show maximum values of 1330 MPa and 2.3% in the V_f range of 10–20%. The decrease in σ_f and ϵ_f in the larger V_f range is due to an increase in the embrittlement tendency. On the other hand, Vickers hardness (H_v) and Young's modulus (E) increase monotonously with increasing V_f. The reason why the strength and elongation increase by the dispersion of nanoscale Al particles is presumably because the nanoscale Al particles with perfect crystalline structure have extremely high strength resulting from the absence of internal defects and act as an effective resistant medium against the shear deformation of the amorphous matrix [30,31]. It is thus found that both strength and ductility of Al-based amorphous alloys increase remarkably through the homogeneous dispersion of the nanoscale Al particles. The highest σ_f value attained by the dispersion of the nanoscale Al particles reaches as high as 1560 MPa which is about three times as high as the highest σ_f of conventional Al-based crystalline alloys. This phenomenon is very important as a new method to develop light-metal base alloys with higher strength and better ductility. The development of the high strength materials by taking advantage of the novel phenomenon has been performed in a collaborate research program between the present authors and some industries.

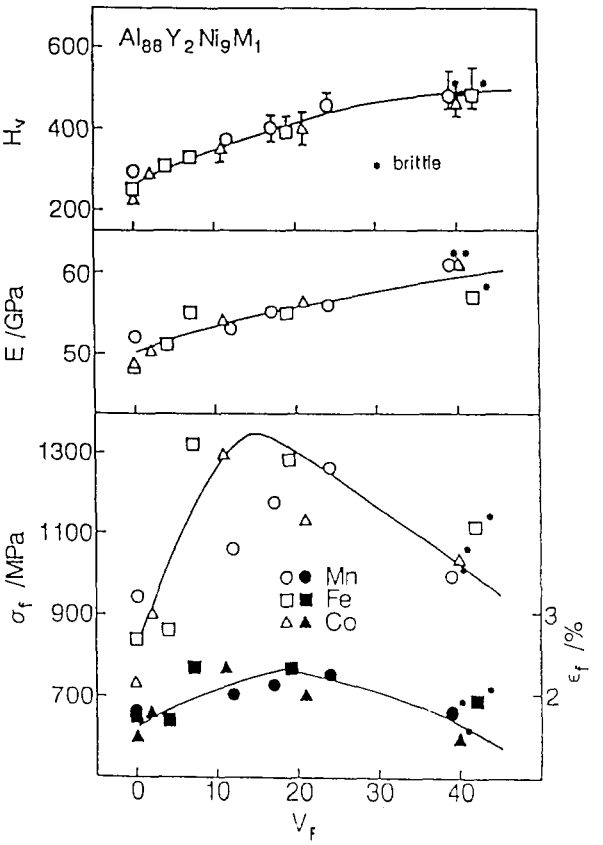

Fig. 6. Mechanical properties as a function of V_f for amorphous $Al_{88}Y_2Ni_9M_1$ (M = Mn, Fe or Co) alloys containing ultrafine Al particles.

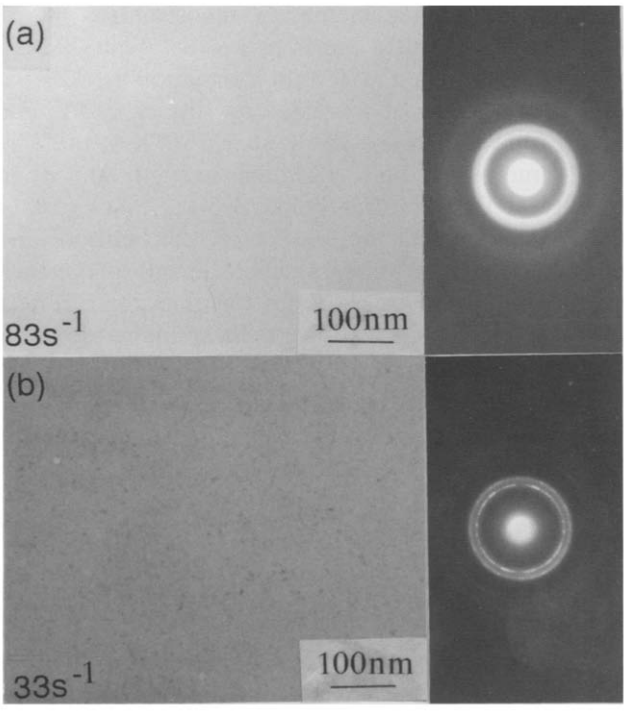

Fig. 5. Bright-field electron micrographs and selected-area diffraction patterns of rapidly solidified $Al_{88}Y_2Ni_9Fe_1$ ribbons. Rotation speed of roller: (a) 83 s^{-1}, (b) 33 s^{-1}.

7. Production of Al-based crystalline alloys with ultrafine grain sizes by extrusion of amorphous powders

Amorphous alloy powders in Al–Y–Ni and Al–Ce–Ni systems have been produced [32] by gas atomization with applied pressures of 4–10 MPa. Although the formation of their amorphous powders is limited to the particle size fraction below 25 μm, the weight ratio is as high as 85%. Thus, Al-based amorphous powders are concluded to be obtained at high production ratios.

The warm extrusion of the Al-based amorphous powders was made in a wide temperature (T_p) range of 500–783 K [33,34]. For instance, the warm extrusion of an $Al_{85}Y_{10}Ni_5$ amorphous powder was possible at temperatures above 540 K. The packing density was 97% at $T_p = 543$ K. With increasing T_p, the density increases and reaches about 100% at T_p above 673 K. The structure of the extruded alloy consists of an amorphous single phase at 543 and 573 K, a duplex structure of amorphous and Al phases at 603 K and mixed phases of $Al + Al_3Y + Al_3Ni$ above 673 K. σ_f and E of the extruded alloy consisting of amorphous and Al phases are 1470 MPa and 145 GPa, respectively, which are two to three times higher than those ($\sigma_{c,y} = 450$ MPa, $E = 71$ GPa) [35] of the conventional 2017 aluminum alloy. As T_p rises to 673 K, $\sigma_{c,f}$ and E decrease to 1220 MPa and 121 GPa, accompanied by the appearance of plastic elongation of 0.5–1.0%. The $\sigma_{c,f}$ value of the extruded alloy is higher than that ($\sigma_f = 1140$ MPa) of a melt-spun $Al_{85}Y_{10}Ni_5$ amorphous ribbon. The increase in $\sigma_{c,f}$ is thought to originate from the dispersion strengthening caused by the homogeneous dispersion of nanoscale Al particles with a size of about 30 nm in the amorphous matrix.

As described above, although the compressive strength of the $Al_{85}Y_{10}Ni_5$ alloy consolidated at temperatures below 673 K is very high, the tensile strength shows lower values ranging from 500 to 700 MPa. The consolidation at temperatures above 703K was carried out with the aim of increasing σ_f. The $Al_{85}Y_{7.5}Ni_{7.5}$ alloy extruded at 783 K has a mixed structure consisting of dispersed Al_3Y and Al_3Ni compounds with a size of about 50 nm in the Al matrix with a grain size of about 0.1 μm. Judging from the previous result [36] that the grain size of a metastable Al-based solid solution in a rapidly solidified $Al_{95}Ce_3Fe_2$ alloy is about 2 μm, it is concluded that the present process consisting of warm extrusion of the amorphous powders is very useful for the formation of the ultrafine mixed structure consisting of fine Al_3Ni and Al_3Y particles embedded in the Al matrix. Figure 7 shows the temperature dependence of σ_f, E, ϵ_p and H_v of the $Al_{85}Y_{7.5}Ni_{7.5}$ and $Al_{91}Y_{4.8}Ni_3Co_{1.2}$ alloys along with the data [35] for commercial 2014-T6 and 7075-T6 alloys. The σ_f, E, ϵ_p and H_v values at room temperature are 940 MPa, 115 GPa, 2.0% and 265, respectively, for the former alloy and 800 MPa, 84 GPa, 3.5% and 220, respectively, for the latter alloy. Although these values decrease with increasing temperature, the high strength level of $\sigma_f = 380$ MPa, $E = 85$ GPa and $H_v = 105$ is kept at 573 K. It is notable that these values are about twice as high as those for commercial Al-based alloys. On the other hand, the ϵ_p increases with increasing temperature and is about 10% at 573 K.

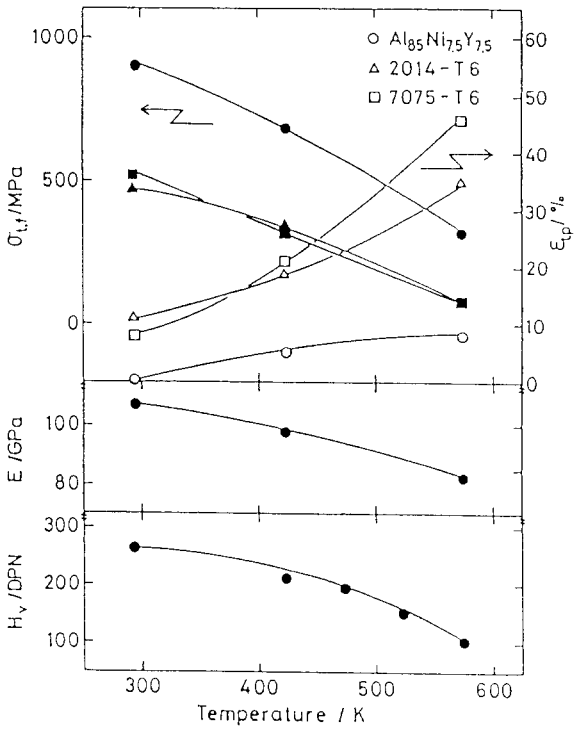

Fig. 7. Changes in mechanical properties with temperature for an $Al_{85}Y_{7.5}Ni_{7.5}$ bulk produced by extrusion at 783 K and an extrusion ratio of 12.

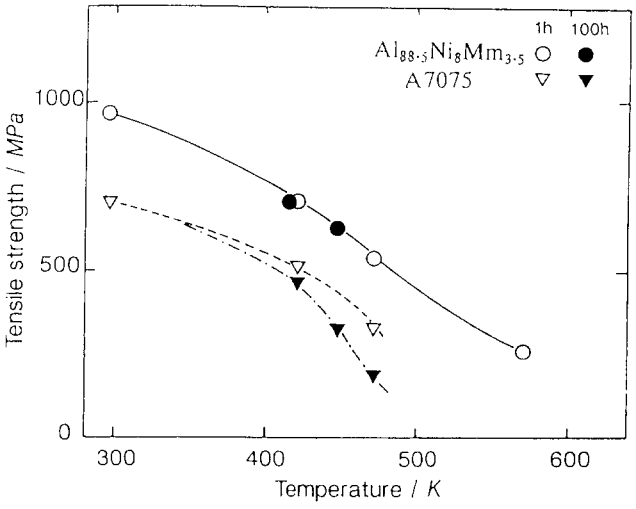

Fig. 8. Temperature dependence of tensile strength for as-extruded $Al_{88.5}Ni_8Mm_{3.5}$ bulks annealed for 1 h and 100 h at each testing temperature. The data for the A7075 alloy are also shown for comparison.

The stability of the high σ_f values against annealing is also shown for the bulky $Al_{88.5}Ni_8Mm_{3.5}$ alloy extruded at 633 K in Fig. 8 [37,38], in comparison with the data [35] for the A7075 alloy. The open and closed circles in the figure represent the data after annealing at each temperature for 3.6 and 360 ks, respectively. σ_f in the case of 3.6 ks annealing for the extruded Al–Ni–Mm bulk is as high as 940 MPa at room temperature which

is much higher than that (700 MPa) for the A7075 alloy. Although σ_f decreases monotonously with increasing temperature, it maintains rather high values of 700 MPa at 423 K and 520 MPa at 473 K. It should be noticed that no appreciable decrease in σ_f is seen even after annealing for 100 h, although the σ_f of the A7075 alloy decreases by 5% at 423 K and by 45% at 473 K. Consequently, in addition to the high tensile strength, the Al–Ni–Mm alloy also has a good heat resistance of tensile strength. The Young's modulus of the extruded Al–Ni–Mm alloy was also as high as 91 GPa. The achievement of the extremely high tensile strength has been contributed to the formation of the mixed structure consisting of homogeneously dispersed Al_3Ni and $Al_{11}(La,Ce)_3$ compounds with a size of 50 nm in an Al matrix with a grain size of 100–200 nm, as shown in Fig. 9. Furthermore, the high σ_f has been roughly evaluated [37] from the sum of the dispersion strengthening and the strengthening due to grain size refinement, as shown in Fig. 10. Such a finely mixed structure cannot be obtained by conventional thermomechanical treatments. The good heat resistance of σ_f for the present alloy is presumably because the strength mechanism is due to the dispersion hardening

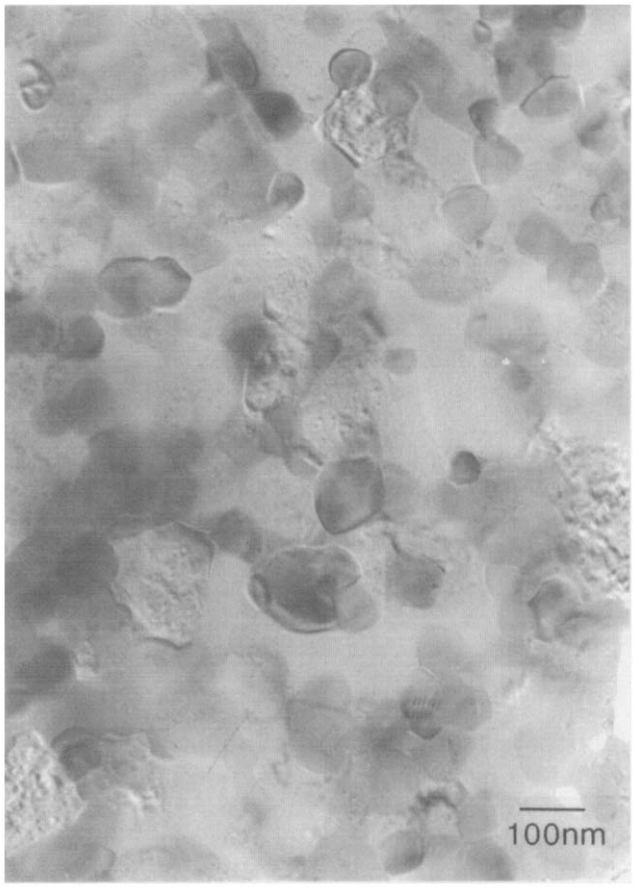

Fig. 9. Bright-field electron micrograph of an as-extruded $Al_{88.5}Ni_8Mm_{3.5}$ alloy.

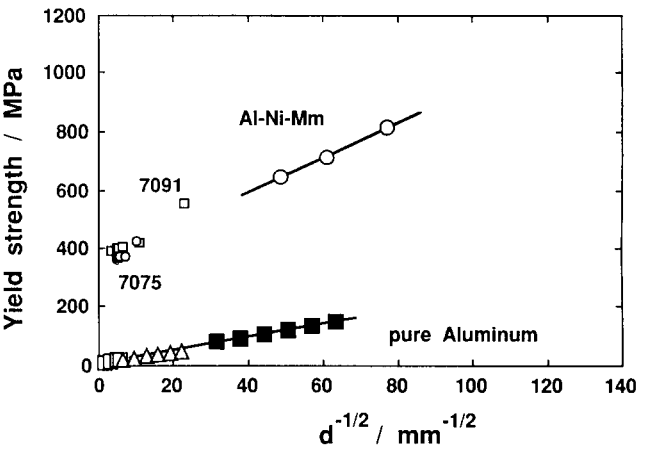

Fig. 10. Hall–Petch relation of the yield strength ($\sigma_{0.2}$) at room temperature for as-extruded $Al_{88.5}Ni_8Mm_{3.5}$ alloys.

by the intermetallic compounds, being different from the result [35] that the strength mechanism for the A7075 alloy is due to the age-hardening mechanism.

The fatigue limit after the cycles of 10^7 for the extruded Al–Ni–Mm alloy was measured to be 330 MPa at 293 K and 196 MPa at 473 K. In order to compare the present fatigue limit with the data for other Al-based alloys, the fatigue limit is plotted in the relation between fatigue limit and tensile strength for Al-based alloys shown in Fig. 11. It can be seen that the fatigue limit is about 1.3 times as high as the highest fatigue limit (260 MPa) [35] for newly developed Al-based alloys made from rapidly solidified powders. It is therefore concluded that both the tensile strength and the fatigue limit for the extruded Al–Ni–Mm alloy are much superior to those for the newly commercialized Al-based alloys developed by using the powder metallurgy technique as well as the conventional Al-based alloys.

It is also expected that a low coefficient of thermal expansion and a high wear resistance are also obtained for the Al–Ni–Mm alloy because of the precipitation of a large amount of Al_3Ni and $Al_{11}(La,Ce)_3$ compounds. Tables 1 and 2 summarize the coefficient of thermal expansion (α) in the temperature range of 423–473 K and the relative wear resistance against S45C, respectively, along with the data [35] for the A6061 and A5056 alloys. The α value is about 20% smaller than that for the conventional Al-based alloys. The wear loss is also about 25% smaller than that for the Al–Si–Mg and Al–Mg base alloys. It is thus concluded that the Al–Ni–Mm alloy has a high wear resistance as well as a low coefficient of thermal expansion.

In addition to the good mechanical properties resulting from the finely mixed structure, the bulk alloys have been reported [39,49] to exhibit marked superplasticity in a high strain rate range of 0.1–10 s^{-1}, as is evidenced from the result shown in Fig. 12 in which the strain rate sensitivity (m value) is above 0.5 and

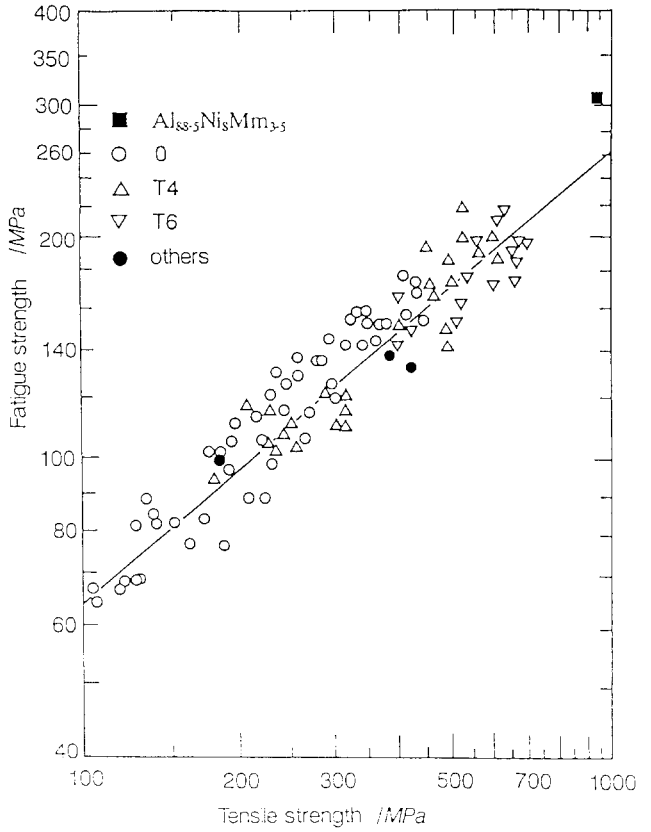

Fig. 11. Relation between fatigue limit after the cycles of 10^7 and tensile fracture strength for an as-extruded $Al_{88.5}Ni_8Mm_{3.5}$ alloy. The data for a conventional Al-based alloy are also shown for comparison.

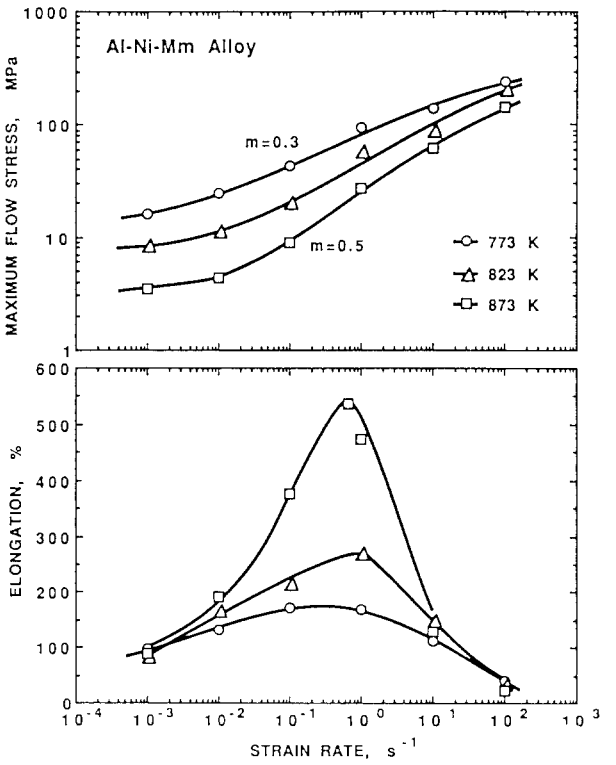

Fig. 12. Variation of flow stress (top) and elongation (bottom) for as-extruded $Al_{88.5}Ni_8Mm_{3.5}$ alloys as a function of strain rate at temperatures between 773 and 873 K.

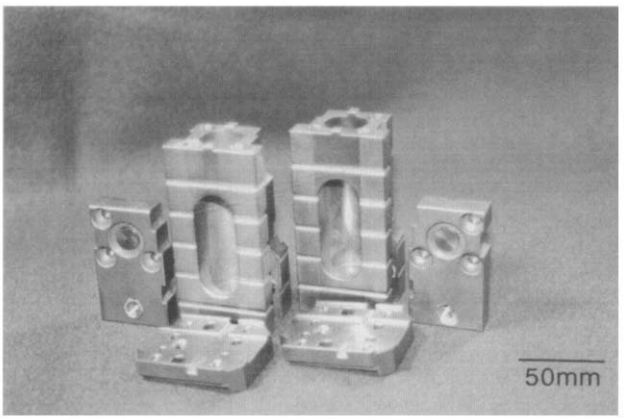

Fig. 13. External appearance of a machinery part made from $Al_{88.5}Ni_8Mm_{3.5}$ powders. The machinery part was produced by extrusion, forging and mechanical polishing.

the maximum elongation reaches as large as 550% at a strain rate of about $1.0\,s^{-1}$.

By utilizing the good superplasticity, the present mixed phase alloys have been deformed into machinery parts with various complicated morphologies. The bulky Al–Ni–Mm alloys produced through the process of extrusion, forging and mechanical polishing have been used [41] as machine parts that are required to have simultaneously high σ_f, high fatigue limit and low coefficient of thermal expansion, as exemplified in Fig. 13. In addition to such machine parts, the new Al-based alloys produced by extrusion of amorphous powders are expected to be used in various application fields where the simultaneous achievement of high strength with light weight, high heat resistance of strength, high fatigue strength, low coefficient of thermal expansion and wear resistance is required.

8. Conclusion

In the framework of the results obtained by the present authors, the formation and mechanical strengths of Al- and Mg-based amorphous alloys were reviewed. The highest σ_f of Al-based alloys is 1250 MPa for the amorphous single phase and 1560 MPa for the mixed structure of nanoscale Al particles embedded in the amorphous matrix. In addition, Mg-based amorphous bulks are produced by the metallic mold casting and the high pressure die casting methods and the σ_f reaches 900 MPa. The σ_f values of these alloys are two to three times as high as the highest value of Al- and Mg-based crystalline alloys developed in the long history of light-metal base alloys. Furthermore, it has been clarified

that the corrosion resistance of the present Al-based amorphous alloys in HCl and NaOH solutions is about 70 and 240 times(16,17), respectively, as high as those for conventional high strength Al-based crystalline alloys. In addition, the corrosion loss in a NaCl solution for amorphous Mg–Ca–Ln alloys is about 30% [42] as small as that for the commercial AZ-91 alloy. The bulky Al-based alloys produced by extrusion of amorphous powders at temperatures above T_x had finely mixed structures consisting of homogeneously dispersed intermetallic compounds in the Al matrix and exhibited high tensile strength and high fatigue limit reaching 940 and 330 MPa, respectively, at room temperature and 520 MPa and 165 MPa, respectively, at 473 K.

In conclusion, the light-metal base amorphous alloys containing Ln elements as a solute element found by the present authors have extremely high values of specific tensile strength and fatigue strength as well as good corrosion resistance. Furthermore, the amorphous alloys can be made in á large scale bulk form by warm working or casting. Accordingly, subsequent development of light-metal base alloys as a new type of high specific strength material can be expected.

References

1 H. Jones, *Aluminum, 54* (1978) 274.
2 C. Suryanarayana, *Rapidly Quenched Metals, A Bibliography, 1973–1979*, Plenum, New York, 1980.
3 A. Inoue, A. Kitamura and T. Masumoto, *J. Mater. Sci., 16* (1981) 1895.
4 A. Inoue, M. Yamamoto, H.M. Kimura and T. Masumoto, *J. Mater. Sci. Lett., 6* (1987) 194.
5 A.P. Tsai, A. Inoue and T. Masumoto, *Met. Trans., 19A* (1988) 1369.
6 A. Inoue, Y. Bizen, H.M. Kimura, T. Masumoto and M. Sakamoto, *J. Mater. Sci., 23* (1988) 3640.
7 A. Inoue, K. Ohtera and T. Masumoto, *Jpn. J. Appl. Phys., 27* (1988) L736.
8 A. Inoue, K. Ohtera, T. Zhang and T. Masumoto, *Jpn. J. Appl. Phys., 27* (1988) L1583.
9 A. Inoue, T. Zhang, K. Kita and T. Masumoto, *Mater. Trans., Jpn. Inst. Met., 30* (1989) 870.
10 A. Inoue, K. Ohtera, A.P. Tsai and T. Masumoto, *Jpn. J. Appl. Phys., 27* (1988) L280.
11 A. Inoue, K. Ohtera and T. Masumoto, *Jpn. J. Appl. Phys., 27* (1988) L1796.
12 A. Inoue, K. Ohtera, K. Kita and T. Masumoto, *Jpn. J. Appl. Phys., 27* (1988) L2248.
13 A. Inoue, M. Kohinata, K. Ohtera, A.P. Tsai and T. Masumoto, *Mater. Trans., Jpn. Inst. Met., 30* (1989) 378.
14 S.G. Kim, A. Inoue and T. Masumoto, *Mater. Trans., Jpn. Inst. Met., 30* (1989) 378.
15 A. Inoue and T. Masumoto, *Bull. Jpn. Inst. Met., 28* (1989) 968.
16 A. Inoue, K. Ohtera and T. Masumoto, *Sci. Rep. Res. Inst. Tohoku Univ., A35* (1990) 115.
17 A. Inoue and T. Masumoto, in L. Arnberg *et al.* (eds.), *Proc. 3rd Int. Conf. on Aluminum Alloys*, Vol. III, SINTEF, Trondheim, Norway, 1992, p. 45.
18 H. Horikiri, A. Kato, A. Inoue and T. Masumoto, *Proc. 8th Int. Conf. on Rapidly Quenched and Metastable Materials*, Sendai, 1993, in press.
19 A. Inoue and T. Masumoto, *J. Jpn. Inst. Light Met., 40* (1990) 453.
20 A. Inoue, N. Matsumoto and T. Masumoto, *Mater. Trans., Jpn. Inst. Met., 31* (1990) 493.
21 Jpn. Inst. Met. (eds.), *Metals Databook*, Maruzen, Tokyo, 1983.
22 A. Inoue, K. Ohtera, A.P. Tsai, H.M. Kimura and T. Masumoto, *Jpn. J. Appl. Phys., 27* (1988), L1579.
23 A. Inoue, *Amorphous Materials*, The 147 Committee, No. 26, Japan Society for the Promotion of Science, Tokyo, 1989, p. 18.
24 E. Matsubara, T. Tamura, Y. Waseda, A. Inoue, M. Kohinata and T. Masumoto, *Mater. Trans., Jpn. Inst. Met., 31* (1990) 228.
25 T. Tamura, Structure of Mg-based amorphous alloys, Master Thesis, Tohoku University, 1991.
26 A. Inoue, A. Kato, T. Zhang, S.G. Kim and T. Masumoto, *Mater. Trans., Jpn. Inst. Met., 32* (1991) 609.
27 T. Masumoto (ed.), *Materials Science of Amorphous Metals*, Ohmu, Tokyo, 1982.
28 Y.H. Kim, A. Inoue and T. Masumoto, *Mater. Trans., Jpn. Inst. Met., 31* (1990) 747.
29 Y.H. Kim, A. Inoue and T. Masumoto, *Mater. Trans., Jpn. Inst. Met., 32* (1991) 331.
30 Y.H. Kim, A. Inoue and T. Masumoto, *Mater. Trans., Jpn. Inst. Met., 32* (1991) 559.
31 Y.H. Kim, A. Inoue and T. Masumoto, *J. Jpn. Inst. Light Met., 42* (1991) 217.
32 A. Inoue, K. Kita, K. Ohtera, H.M. Kimura and T. Masumoto, *J. Mater. Sci. Lett., 7* (1988) 1287.
33 A. Inoue, K. Ohtera and T. Masumoto, in ed. N. Igata *et al.* (eds.), *Proc. 1st Jpn. Inst. SAMPE Symposium*, Nikkan Kogyo Shimbun, Tokyo, 1989, p. 7.
34 A. Inoue and T. Masumoto, *Mater. Sci. Eng., A133* (1991) 6.
35 A.K. Vasudevan and R.O. Doherty, *Aluminum Alloys*, Academic Press, London, 1989.
36 A. Inoue, H. Yamaguchi, M. Kikuchi and T. Masumoto, *Sci. Rep. Res. Inst. Tohoku Univ., A35* (1990) 101.
37 K. Ohtera, A. Inoue, T. Terabayashi, H. Nagahama and T. Masumoto, *Mater. Trans., Jpn. Inst. Met., 33* (1992) 775.
38 K. Ohtera, K. Kita, N. Nagahama, A. Inoue and T. Masumoto, in L. Arnberg *et al.* (eds.), *Proc. 3rd Int. Conf. on Aluminum Alloys*, SINTEF, Trondheim, Norway, 1992, p. 58.
39 K. Higashi, T. Mukai, S. Tanimura, A. Inoue, T. Masumoto, K. Kita, K Ohtera and J. Nagahora, *Scripta Met., 26* (1992) 191.
40 K. Higashi, T. Mukai, S. Tanimura, A. Inoue, T. Masumoto and K. Ohtera, *J. Alloys Comp., 193* (1993) 29.
41 K. Ohtera, T. Terabayashi, H. Nagahama, A. Inoue and T. Masumoto, *J. Jpn. Soc. Powder Powder Metall., 38* (1991) 953.
42 A. Kato. H. Horikiri, A. Inoue and T. Masumoto, *Proc. 8th Int. Conf. on Rapidly Quenched and Metastable Materials*, Sendai, 1993, in press.